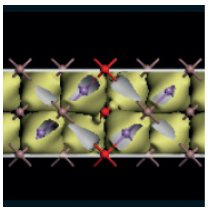

Session: Phonon Properties and Thermal Transport

(Invited) Anderson-like localization of phonon in nano-structures

Y Chalopin[1], S Mayboroda[2] and M Filoche[3]

[1]Ecole CentraleSupelec, France, [2]University of Minnesota, USA, [3]Ecole Polytechnique, France

Based on a recent theory of wave localization and the development of a mathematical tool (the localization landscape) we propose an approach that predicts the localization of thermal phonons in disordered lattices. An analogy between the Schrödinger equation and the classical equation of motion is introduced to demonstrate that localization of thermal energy in phonon systems arises from atomic disorder through which the localization landscape can be revealed. This approach, illustrated on disordered graphene, provides a powerful framework for engineering heat conduction in nanostructures using wave effects.

Thermionic cooling devices based on AlGaAs/GaAs heterostructures

M Bescond[1], D Logoteta[1], N Cavassilas[1], A Yangui[2], K Hirakawa[2] and M Lannoo[1]

[1] CNRS IM2NP, France, [2]University of Tokyo, Japan

Efficient cooling devices in nanoelectronics and optoelectronics is a matter of urgency. For in- stance, it is well-recognized that self-heating of microprocessors is one of the fundamental limit to system performance [1]. Recently, nanostructured devices have attracted broad interest since they have enhanced thermoelectric effects with respect to their bulk counterparts [2]. The present work theoretically investigates thermionic cooling devices based on AlGaAs/GaAs heterostructures. To do so, we couple self-consistently the non-equilibirum Green's function (NEGF) equations for electrons with 1D-Poisson equation for electrostatic and 1D- heat equation [3], [4]. Phonon scattering in the elec- tron transport is described *via* the concept of self-energy in the self-consistent Born approximation (SCBA). It includes interactions with acoustic and non-polar optical phonons as well as long range polar optical interactions of the Fro¨hlich type treated within a diagonal (*i.e.* local) approach [5].

Figure 1 represents the studied semiconductor het- erostructure refrigerator (SHR) initially proposed in Ref.[6] which couples tunneling injection with thermionic extraction. The cold electrons are in- jected into the active region by resonant tunneling through a potential barrier, while the hot electrons are removed from the active region by thermionic emission over a thicker barrier that serves as a thermal wall to reduce the heat backflow. Since the left access region cools while the right one heats up, the central region acts then as an energy-selective filter [7].

Figure 2 shows the current characteristics obtained for three different temperatures enforced at the contacts without (empty symbols) and with (solid symbols) the treatment of the heat equation. We can see that the self-heating inside the active region has almost no influence on the current even at higher temperatures. However, the two physical phenom- ena described in Figure 1, namely the resonant tun- neling and the thermionic emission above the thick barrier are clearly visible in the current spectrum (Fig.3). In particular we see in Figure 4 that the current injected from the left part of the active region corresponds to the energy of the resonant state in the central GaAs quantum well.

Moreover, as shown in Figure 5, the electronic heat power density (*i.e.* the power transferred locally between the electrons and the lattice) is negative in the left region (the lattice is cooled by the electron current) and peaked at the position of the resonant level.

Acoustic phonons having a higher group velocity than their optical counterparts they are responsi- ble of heat transport. Figure 6 shows the acoustic phonon temperature along the device. As expected it decreases in the left region while it increases in the right side. The considered SHR actually acts as a thermionic cooling device. This work quantifies the heat removal by the electric current due to the resonant-tunneling thermionic process. A numerical analysis will be performed in order to optimize the performances of the device and to reach the highest thermionic cooling efficiency.

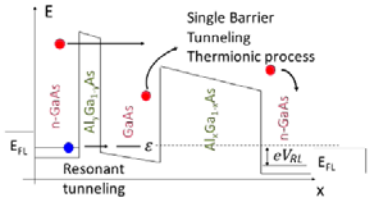

Fig. 1. Schematic representation of the heterostructure. The thicknesses of the left and right n-GaAs regions are equal to 150 nm and 60 nm respectively with a doping of 10^{18}cm^{-3}. The AlGaAs barriers have a thickness of 2.4 nm and 150 nm respectively. The Al mole fractions are $y = 0.2$ and $x = 0.1$. The GaAs quantum well thickness is 4.8 nm.

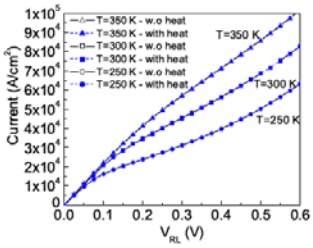

Fig. 2. Current characteristics for three temperatures: T = 350 K (triangles), 300 K (squares), and 250 K (circles). Empty symbols corresponds to the results obtained without including the coupling with the heat equation while the solid symbols are obtained with the effect of heat equation.

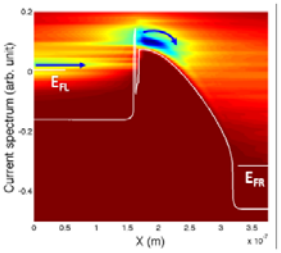

Fig. 3. Current spectrum obtained at T = 350 K and V_{RL}=0.3 V. Fermi levels of left and right contacts are also represented. Arrows indicate the main current flux in the left access region and above the barrier, highlighting the physical processes represented in Figure 1.

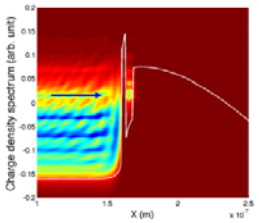

Fig. 4. Charge density spectrum corresponding to the current of Fig. 3. The current injected from the left contact clearly aligns with the resonant level of the central GaAs quantum well.

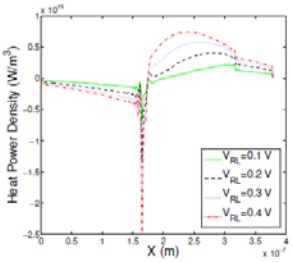

Fig. 5. Heat power density along the structure obtained at T = 350 K for various biases V_{RL}. Positive and negative components are well separated spatially by the resonant level.

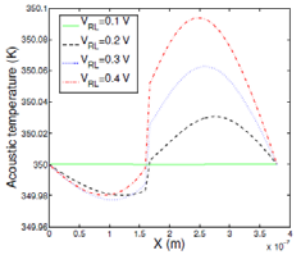

Fig. 6. Acoustic phonon temperature profiles corresponding to the heat power density of Fig. 5. The temperature cools by 20 mK in the left side and increases by almost 90 mK in the right side.

[1] R. Rhyner *et al.*, *Nano Lett.* 16, 1022 (2016).
[2] J.T. Muhonen *et al.*, *Rep. Prog. Phys.* 75, 046501 (2012).

[3] R. Kim *et al.*, *J. Appl. Phys.* 110, 03451 (2011).
[4] M. Pala *et al.*, *J. Appl. Phys.* 117, 084313 (2015).
[5] M. Moussavou, M. Bescond *et al.*, under preparation (2017).
[6] K. A. Chao *et al.*, *Appl. Phys. Lett.* 87, 022103 (2005).
[7] T. E. Humphrey *et al.*, *Phys. Rev. Lett.* 89, 116801 (2002).

DFT/NEGF study of discrete dopants in Si/GaAs 3D FETs including phonon scattering and self-heating

L Wilson[1], A Martinez[1], A Price[1] and R Rurali[2]

[1]Swansea University, UK, [2]Institut de Ciència de Materials de Barcelona, Spain

Si FinFET nanowire transistors have been in production since 2010 and exhibit the promise of superior electrostatic and better performance than the planar MOSFET counterpart. As the size of the active regions of devices continues to be scaled down to nanometre dimensions, the number and location of a few impurities dramatically affect device performance. Tunnelling and confinement combined by strong local electrostatic potential invalidate the use of semi- classical models such as the drift-diffusion and Monte Carlo methods. The lack of validity of these methodologies to sub 10 nanometre dimensions is a direct consequence of the wave nature of the electron. Substantial work on discrete dopants has been carried out using a discrete point charge model in the NEGF formalism [1]. The density produced by this point model is mostly spherically symmetric or slightly deformed by the effective mass tensor. However, the wavefunction of the electron/hole occupying the dopant atom exhibits a tetrahedral symmetry and a shape dictated by the atomistic distribution of the surrounding. This can be seen in Fig. 1 and 2, which shows the absolute value of the wavefunction corresponding to an impurity embedded in Si and GaAs atom supercells. In the case of silicon, the dopant atom is Phosphorus and in the GaAs the dopant atom is Silicon. There is a concern of how reliable this point charge model is and what are the differences of using a more accurate description of the dopant and how much the I-V characteristic is changed by the use of this model. In this work, using non-equilibrium Greens Function (NEGF) formalism, we calculated the transfer characteristics of Si and GaAs nanowire transistors with a dopant in the middle of the channel [2]. The device has a 2.2 mm2 cross-section and a 6 nm channel length. The self- consistent electrostatic energy is shown in Fig. 4. We model the dopant atoms as a point charge, see Fig. 4, and also as a charge which reflects the DFT electron density. Scattering and self-heating are included. The calculation of the DFT dopant wavefunction is carried out with the Siesta code [3], using a supercell of 512 atoms. The ID-VG characteristics for the Si and GaAs devices are shown in Fig. 3, all simulations are done at VD = 0.4 V. In general, the current difference between the two dopant models is small. However, the difference is large in the case of GaAs. This difference can be attributed to the slight decrease in the source drain barrier height induced by the point charge. This effect can be observed by comparing the subbands in Fig. 5 and Fig. 6. These figures show the current spectrum and the first subbands for the 3 lowest Valleys of GaAs. Fig. 7 and 8 show the current spectra for the Si Device with DFT distributed charge at low and high drain. At low gate, the electron system heats up in the source and cools down at the drain, however at high gate bias the electron system is more efficient to dissipate the energy as the cooling of the electron system starts at the source- channel interface. It should be noted that for these devices there is a substantial amount of source to drain tunnelling. This can be observed in all the figures showing the current spectrum.